

---

# Navigating Conflicting Views: Harnessing Trust for Learning

---

**Joeqing Lu**  
Monash University  
jueqing.lu@monash.edu

**Lan Du \***  
Monash University  
lan.du@monash.edu

**Wray Buntine**  
VinUniversity  
wray.buntine@vinuni.edu.vn

**Myong Chol Jung**  
Monash University  
david.jung@monash.edu

**Joanna Dipnall**  
Monash University  
jo.dipnall@monash.edu

**Belinda Gabbe**  
Monash University  
belinda.gabbe@monash.edu

## Abstract

Resolving conflicts is essential to make the decisions of multi-view classification more reliable. Much research has been conducted on learning consistent informative representations among different views, assuming that all views are identically important and strictly aligned. However, real-world multi-view data may not always conform to these assumptions, as some views may express distinct information. To address this issue, we develop a computational trust-based discounting method to enhance the existing trustworthy framework in scenarios where conflicts between different views may arise. Its belief fusion process considers the trustworthiness of predictions made by individual views via an instance-wise probability-sensitive trust discounting mechanism. We evaluate our method on six real-world datasets, using Top-1 Accuracy, AUC-ROC for Uncertainty-Aware Prediction, Fleiss' Kappa, and a new metric called Multi-View Agreement with Ground Truth that takes into consideration the ground truth labels. The experimental results show that computational trust can effectively resolve conflicts, paving the way for more reliable multi-view classification models in real-world applications. <sup>2</sup>

## 1 Introduction

Multi-View Classification (MVC) plays a critical role in deep learning by greatly enhancing the ability to make accurate decisions through integrating the multi-source information. Its effectiveness has been verified with the successful application in many domains such as autonomous driving [37] and AI-assisted medical diagnostic systems [21]. Most of the existing studies on MVC rely on the assumption that data from different views are consistently of good quality and informative with regard to the ground truth [24, 39, 36]. Nevertheless, this assumption may not always be valid in real-world scenarios. Substantial variations in the quality of data from different views can produce contradictory results, thereby undermining the reliability of the model's predictions.

A possible solution for resolving conflicts is to project data from different views into a latent common space [10, 33, 2, 11], and then draw a combined representation from the latent space for the classification. This is achieved by integrating essential features via weighting schemes, such as attention mechanisms [41] and weighted fusion [1, 38]. These methods typically assign higher weights to more informative views or features, thus reducing the impact of potential conflicting or noisy information. Although these methods have achieved promising results in MVC, their focus

---

\*Corresponding author

<sup>2</sup>We will release our codes once our paper is accepted.

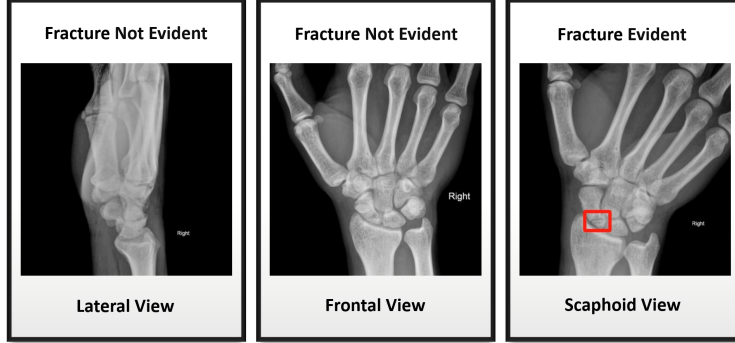


Figure 1: Conflict in Medical Imaging. Fracture (red box) is evident in one view, but not evident in another two. Adapted from a case study by [27].

on the combined joint representation can be a limitation. Solely relying on the joint representation hinders the capacity to thoroughly grasp information provided by different views. In contexts such as medical diagnosis, characterized by heterogeneous data sources from various views of medical imaging (e.g., lateral, frontal and scaphoid views in X-rays (Figure 1) ), it’s crucial to thoroughly analyze and comprehend each view before establishing a comprehensive diagnosis, as each view often offers unique information [31].

Existing approaches to resolve conflicts build neural networks to generate view-specific predictions and then combine view-specific predictions together. As a prime example, the evidence-based framework is emerging as a promising approach, offering a reliable means for the final fusion stage. Within this framework, evidence acts as a metric of endorsement for the associated predicted label, and the evidence is collected through view-specific neural networks. Subsequently, evidence from diverse viewpoints is fused, considering their respective epistemic uncertainties. However, there may exist cases where the view-specific information is not well aligned with the ground truth, resulting in misleading predictions with high confidence (low uncertainty). For example, as shown in Figure 1, Fracture is evident in the scaphoid view but not evident in others. A pioneering work [36] based on the evidence framework tried to resolve conflicts by minimizing the degree of conflict loss. However, this approach may inadvertently converge towards incorrect predictions, potentially leading to unstable performance.

In this work, we take a significant step further: leveraging the evidence-based framework, we propose a new computational trust based opinion fusion method to resolve potential conflicts in MVC. Specifically, the computational trust is modelled through an evidence network that operates on a view-specific and sample-wise basis. Drawing upon the principle of trust discounting in subjective logic, it evaluates the trustworthiness of view-specific predictions generated by existing evidence-based frameworks, such as Evidential Deep Learning (EDL) [29]. Within the proposed method, each view-specific evidence is transformed into a degree of trust using the Binomial opinion theory [15]. These degrees of trust are then utilized to establish uncertainty and a trust-aware opinion, ultimately facilitating the generation of reliable predictions. In summary, the contributions of this paper include:

1. We present a novel learnable trust-discounting mechanism to extend the widely-used evidence-based trustworthy MVC framework, enhancing its conflict resolution capabilities. Drawing from the Binomial opinion theory within subjective logic, it operates on a view-specific and instance-wise basis, adeptly resolving conflicts among views through a probability-sensitive trust discounting rule;
2. We develop a stage-wise training strategy to optimize the parameters of the proposed mechanism, which works robustly on different datasets;
3. We conduct extensive experiments on six real-world datasets, showing that our method outperforms the existing trusted MVC methods based on evidential deep learning, particularly on the datasets exhibiting large discrepancy among view-specific predictions. In addition, our method can also enhance the consistency among opinions derived from different views.

Table 1: Illustration of fusing conflicting opinions with BCF, A-CBF and ABF

	Source Opinions		Fused Opinions			Trust Fusion		
	$\tilde{\omega}^1$	$\tilde{\omega}^2$	BCF	A-CBF	ABF	$\tilde{\omega}^1$	$\tilde{\omega}^2$	TD+BCF
$b_1$	0.67	0.1	0.387	0.391	0.385	0.9	0.0	0.56
$b_2$	0.2	0.2	0.222	0.203	0.200	0.0	0.9	0.19
$b_3$	0.1	0.67	0.387	0.391	0.385	NA	NA	0.16
$u$	0.03	0.03	0.004	0.015	0.030	0.1	0.1	0.09

## 2 Trust-discounted Fusion for Conflict Resolving

Given training data  $\mathcal{D} = \{\{\mathbf{x}_i^v\}_{v=1}^V, y_i\}_{i=1}^N$  where  $N$  is the number of training data, each instance  $\mathbf{x}_i$  has  $V$  views, ground truth label  $y_i$  and an one-hot encoded label  $\mathbf{y}_i$  (i.e., for a  $K$ -class classification problem,  $\mathbf{y}_{i,k}$  is 1 if  $k$  is the index of ground truth label for  $i$ -th instance, otherwise it is 0). The task of MVC is to learn a function  $f$  that maps  $\{\mathbf{x}_i^v\}_{v=1}^V$  to  $\mathbf{y}_i$ .

### 2.1 Preliminaries on Evidence Theory for MVC

The evidence-based framework applies Subjective Logic (SL) to the  $K$ -class classification problem by assigning belief masses to individual class labels and computing epistemic uncertainty for the generated belief masses. The formulation links the evidence collected from instance view-specific observation to the concentration parameter of the Dirichlet Distribution. Let  $f_\theta^v(\cdot)$  denote the view-specific neural network for evidence generation, where the view-specific evidence for an instance is  $e^v = f_\theta^v(\mathbf{x}^v)$ , the association between the evidence and the Dirichlet parameters is simply  $\alpha_k = e_k + 1$  [29, 8]. The belief mass on class label  $k$ , denoted as  $b_k$ , and uncertainty  $u$  are subject to the additive requirement, i.e.,  $u + \sum_{k=1}^K b_k = 1$ . With respect to MVC, the view-specific belief mass  $b_k^v$  and uncertainty  $u^v$  can then be computed as

$$S^v = \sum_{k=1}^K \alpha_k^v, \quad b_k^v = \frac{e_k^v}{S^v} = \frac{\alpha_k^v - 1}{S^v}, \quad u^v = 1 - \sum_{k=1}^K b_k^v = \frac{K}{S^v} \quad (1)$$

To generate the final prediction, SL models the view-specific predictions as multinomial opinions, denoted as  $\omega^v = [\mathbf{b}^v, u^v, \mathbf{a}^v]$ , with  $\mathbf{a}^v$  being the base rate (i.e., a prior probability distribution over classes, generally a discrete uniform distribution), and then combine them together with an appropriate belief fusion rules based on the context [17]. The Belief Constraint Fusion (BCF) [17], an extension of Dempster-Shafer combination rule [30], was first adopted by [8] in trusted MVC. Other fusion rules, such as Aleatory Cumulative Belief Fusion (A-CBF) [25] and Averaging Belief Fusion (ABF) [36] have also been explored. We stay with BCF in our experiments based on the empirical results. For fusing different opinions, i.e.,  $\omega = \omega^1 \oplus \omega^2 \oplus \dots \omega^V$  from  $V$  views, the fusion rule of BCF among two views can be formulated as follows:

$$b_k = \frac{1}{1-C} (b_k^1 b_k^2 + b_k^1 u^2 + b_k^2 u^1), \quad u = \frac{1}{1-C} u^1 u^2 \quad (2)$$

where  $C = \sum_{i \neq j} b_i^1 b_j^2$  is the normalization factor. Applying Eq. (2) iteratively will derive the final fused opinion from the  $V$  views, and the order does not affect the combined result [15]. For the fused opinion  $\omega$ , we can derive the parameters of the Dirichlet  $\alpha_k$  by reversing the computation of Eq. (1).

An alternative representation for BCF is based on combining the evidence, from which the opinions  $[\mathbf{b}, u, \mathbf{a}]$  can be derived:

$$e_k = e_k^1 + e_k^2 + \frac{e_k^1 e_k^2}{K} \quad (3)$$

Note that A-CBF corresponds to the case where the third term is removed, and thus for the Dirichlet likelihood can be interpreted as Bayesian updating assuming independent evidence.

### 2.2 Conflict Resolving by Trust Discounting

We realize conflicts can happen when view-specific opinions express conflicting preferences with similar level of confidence, leading to inaccuracies in the combined opinion. Based upon this, we define the conflict problem as follows:

**Definition 1** (Conflicts within Multi-view Learning). *For a  $K$ -class multi-class classification problem, the view-specific models give confident yet opposite opinions for a given data instance.*

Table 1 presents a scenario with a two-view instance for 3-class classification, illustrating the concept of conflict views. Conflict arises for such a data instance  $\{\mathbf{x}^v\}_{v=1}^2$  with the ground label  $y = 1$ , when the opinions are  $\mathbf{b}^1 = [0.67, 0.2, 0.1]$  and  $u^1 = 0.03$ , alongside  $\mathbf{b}^2 = [0.1, 0.2, 0.67]$  and  $u^2 = 0.03$ . Existing fusion approaches, as depicted in Table 1, struggle to provide a clear and accurate final prediction, as they all generate the same belief mass for labels 1 and 3 due to the confidence of both opinions with low uncertainty.

Instead, we utilize the principle of Trust Fusion (TF) by Trust Discounting (TD) [18] to resolve conflicts. The basic idea of TD is to discount information provided by an individual view as a function of trust in that view. It can be used to weigh the current view-specific opinion according to the degree of trust, thus guiding the fusion process to generate more reliable prediction. Here we present a Probability-sensitive Trust Discounting rule, as show in Eq. (4), and use it in an instance-wise manner in our experiments, This rule computes the trust degree by the expect value of projected Beta distribution  $\beta(\alpha_1, \alpha_2)$  (i.e.,  $p_t = \frac{\alpha_2}{\alpha_1 + \alpha_2}$ ) for each individual instance on each view, following Binomial opinion theory. It is noteworthy that other choices to compute the trust degree are also possible, such as Uncertainty Favouring Discounting and Opposite Belief Favouring Discounting [16]. They can be easily integrated into our framework.

To distinguish different types of opinions, we modify notations used in the previous section. Concretely, the opinions before applying trust fusion, is often referred to as Functional (Trust) Opinion, denoted as  $\hat{\omega}$ , in the form of multinomial opinion discussed in Section 2.1. Meanwhile, the opinion used for discounting is known as the Referral (Trust) Opinion, denoted as a Binomial opinion  $\check{\omega}$ , and  $\check{\omega}$  is used to indicate the trust-discounted opinion. From [15], the discounting rule is defined as:

**Definition 2** (Instance-wise Probability-Sensitive Trust Discounting). *For each view of each individual instance, the trust-discounted opinion is defined as*

$$\check{\omega} = \check{\omega} \otimes \hat{\omega} = \begin{cases} \check{\mathbf{b}} = \check{p}_t * \hat{\mathbf{b}}, \\ \check{u} = 1 - \check{p}_t * \left( \sum_{k=1}^K \hat{b}_k \right), \\ \check{\mathbf{a}} = \hat{\mathbf{a}}. \end{cases} \quad (4)$$

where  $\otimes$  indicates the trust discounting operator, and the scalar probability  $\check{p}_t$  denotes the degree of trust, representing how much we are confident with the information given by the view-specific model. In contrast,  $\check{p}_d = \frac{\check{\alpha}_1}{\check{\alpha}_1 + \check{\alpha}_2}$  denotes the degree of distrust, and is subject to the constraint  $\check{p}_t + \check{p}_d = 1$ .

Note this corresponds to updating the Dirichlet evidence by  $\check{e}_k = \frac{\check{p}_t \hat{u}}{1 - \check{p}_t + \check{p}_t \hat{u}} \hat{e}_k$ . Given Eq. (4), we fuse the trust-discounted opinions from  $V$  views of  $i$ -th instance with BCF by:

$$\bar{\omega}_i = \check{\omega}_i^1 \oplus \check{\omega}_i^2 \oplus \dots \oplus \check{\omega}_i^V = (\check{\omega}_i^1 \otimes \hat{\omega}_i^1) \oplus (\check{\omega}_i^2 \otimes \hat{\omega}_i^2) \oplus \dots \oplus (\check{\omega}_i^V \otimes \hat{\omega}_i^V) \quad (5)$$

In the presence of conflicting opinions, the estimated uncertainty is expected to increase, even if the uncertainty associated with the prediction of each individual view is small. However, the uncertainty of fused opinion given by the fusion rules mentioned above is always under-estimated, thus inconsistent with the generated beliefs, as shown by the example in Table 1. With the trust-discounting rule, conflicts can be effectively solved within the evidential learning framework, ensuring theoretically-guaranteed better fusion, as demonstrated by Proposition 1 and Proposition 2 together with the example in Table 1. Specifically, Proposition 1 illustrates that our TD rule consistently enhance classification accuracy, while Proposition 2 establishes that TD corrects and adjusts the under-estimated uncertainty. The following propositions provide theoretical analysis of the proposed TD rule, and their detailed proof can be found in Appendix A.4.

**Proposition 1.** *Probability Sensitive Trust-Discounting maximizes the belief mass of the Ground truth label after BCF, under the assumption that at least one view's prediction is correct.*

**Proposition 2.** *The combined opinion generated by BCF with trust discounting for conflicting views, will exhibit greater uncertainty than obtained through fusion with non-discounted functional opinions.*

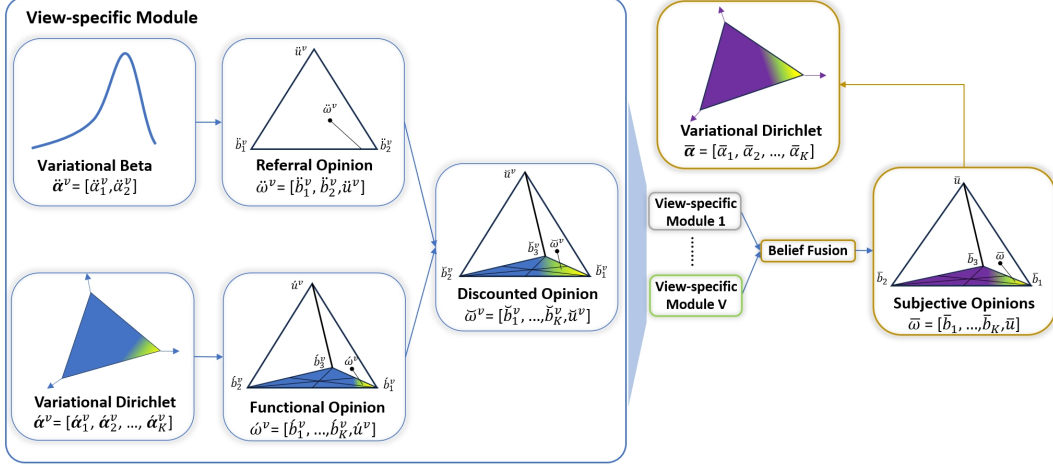


Figure 2: The Trust Discounting Mechanism based Multi-view Evidential Framework

### 2.3 Learning to Form Opinions

Similar to the generation process of a functional opinion, we construct another view-specific evidence network parameterized by  $\hat{\theta}$ , for outputs referral evidence  $\hat{e}$ , i.e.,  $\hat{e}_i^v = f_{\hat{\theta}}^v([\mathbf{x}_i^v, \mathbf{b}_i^v])^3$ . Figure 2 depicts our TF rule along with entire evidence-based learning framework.

For optimizing network parameters, we propose a stage-wise training algorithm (Algo. 1), drawing inspiration from [7], to avoid any potential numerical instability problems during training. In the proposed training algorithm, we follow [29, 8, 9, 36], and use the following loss term  $L(\alpha)$ <sup>4</sup> to optimize the parameters of the Dirichlet distribution for where it applies,

$$L(\alpha) = L_{ace}(\alpha) + \lambda_o D_{KL}[\text{Dir}(\mathbf{p}|\tilde{\alpha})||\text{Dir}(\mathbf{p}|\mathbf{1})] \quad (6)$$

where  $\tilde{\alpha} = \mathbf{y} + (1 - \mathbf{y}) \odot \alpha$  is the Dirichlet parameters after removing non-misleading evidence from predicted parameters  $\alpha$ , and  $\mathbf{p}$  is the projected probability, i.e.,  $\mathbf{p} = \frac{\alpha}{\sum}$ .  $\odot$  is the element-wise product and  $\lambda_o$  is the annealing factor. Specifically, in the proposed algorithm, we apply Eq. (6) to the Dirichlet parameters with regard to all functional opinions (i.e.,  $\{\hat{\alpha}_i^v\}_{v=1}^V$ ) at stage-2a. At stages 2b and 3, we apply this loss term only to the parameters of the Dirichlet distribution concerning the BCF combined opinion (i.e.,  $\bar{\alpha}_i$ ). Please note that for the BCF combined opinion, both the functional opinion and the referral opinion are required. Therefore, when applying back-propagation (BP) with regard to the combined opinion, there will be gradients for both the referral network and the functional network. We update different types of networks at different stages. For example, we only update the functional network at stage-2b and only update the referral network at stage-3.

Since the parameters of the referral network are randomly initialised at the beginning, we adopt the ace loss from above with a new smoothed label to warm-up those parameters. For each  $i$ -th instance on  $v$ -th view, the hard label  $z_i^v$  is generated by

$$z_i^v = \begin{cases} 1 & \text{if } \hat{y}_i^v = y_i \\ 0 & \text{otherwise} \end{cases} \quad (7)$$

Following [26], we apply label smoothing with smoothing factor  $\eta = 0.9$  to the hard label. The association between one-hot encoded hard label  $\mathbf{z}_i^v$  of target  $z_i^v$  and smooth label is  $\hat{\mathbf{z}}_i^v = \mathbf{z}_i^v \odot \eta + \eta/2$ . since the smoothed label could provide training signals for neurons of both target and non-target labels, we simply adopt  $\sum_v L_{ace}(\hat{\alpha}_i^v)$  with smoothed labels  $\{\hat{\mathbf{z}}_i^v\}_{v=1}^V$  in the first warm-up stage, and

$$L_{ace}(\hat{\alpha}_i^v) = \sum_{j=1}^2 \hat{\mathbf{z}}_{ij}^v (\psi(\hat{\alpha}_{i1}^v + \hat{\alpha}_{i2}^v) - \psi(\hat{\alpha}_{ij}^v)) \quad (8)$$

where  $\hat{\alpha}_i^v$  is the parameters of Beta distribution of referral opinion and  $\psi$  is the digamma function.

<sup>3</sup>We used Bi-Linear layer instead of Dense/Linear Layer in our experiments.

<sup>4</sup>The closed form of ace loss and KL-divergence loss will be shown in Appendix A.5.

### 3 Related Work

---

**Algorithm 1:** Algorithm for Training and Testing

---

**Input:** Multi-view dataset:  $\mathcal{D} = \{\{\mathbf{x}_i^v\}_{v=1}^V, y_i\}_{i=1}^N$ .  
*/\*Training\*/*

**Initialize:** Initialize the parameters  $\hat{\theta}$  of the Functional networks; initialize the parameters  $\ddot{\theta}$  of the Referral networks.

*/\*Stage-1 Warm-up Referral Network\*/*

**for** *minibatch* **do**

**for**  $v = 1 : V$  **do**

$\ddot{e}^v \leftarrow$  Referral Evidential network batch output;

    Obtain  $\ddot{\alpha}^v \leftarrow \ddot{e}^v + 1$  ;

**end**

  Obtain overall loss by summing losses calculated by Eq. (8) of all  $\{\ddot{\alpha}^v\}_{v=1}^V$  ;

  Update the parameters  $\hat{\theta}$  by gradient descent with the loss from above;

**end**

*/\*Stage-2 Update Functional Network\*/*

**for** *minibatch* **do**

*/\*Substage-2a\*/*

**for**  $v = 1 : V$  **do**

$\acute{e}^v \leftarrow$  Functional Evidential network batch output;

    Obtain  $\acute{\alpha}^v \leftarrow \acute{e}^v + 1$  ;

**end**

  Obtain overall loss by summing losses calculated by Eq. (6) of all  $\{\acute{\alpha}^v\}_{v=1}^V$  ;

  Update the parameters  $\hat{\theta}$  by gradient descent with the loss from above;

*/\*Substage-2b\*/*

**for**  $v = 1 : V$  **do**

$\ddot{e}^v \leftarrow$  Referral Evidential network batch output;

$\acute{e}^v \leftarrow$  Functional Evidential network batch output;

    Obtain  $\ddot{\omega}^v$  and  $\acute{\omega}^v$  by Eq. (1) with  $\ddot{e}^v$  and  $\acute{e}^v$ , respectively ;

**end**

  Obtain joint opinion  $\bar{\omega}$  by Eq. (5) and  $\bar{\alpha}$  of this opinion by reversing Eq. (1);

  Obtain loss by Eq. (6) with  $\bar{\alpha}$  and update the parameters  $\hat{\theta}$  with gradient descent;

**end**

*/\*Stage-3 Adjust Referral Network\*/*

By repeating Stage-2b only and update  $\ddot{\theta}$  instead of  $\hat{\theta}$ ;

*/\*Stage-4 Adjust Functional Network\*/*

By repeating entire Stage-2;

**Output:** Functional and Referral networks parameters.

*/\*Test\*/*

Calculate the joint belief and the uncertainty mass through fusing discounted opinions by Eq. (5).

---

**Multi-View Classification** leverages multiple data sources, offering varied perspectives on the same object, to enhance the classification performance. Recent advancements in MVC have focused on generating noise-robust representations through cluster-based [14, 34, 40], self-representation-based [12], and partially view-aligned [35, 13] methods, harnessing the expressive power of deep neural networks. However, noise-robust representations may not fully resolve conflicts in opinions for a given data instance, as they lack a mechanism to quantify the trustworthiness of each view. Our method addresses this limitation by introducing an evidence network that evaluates the reliability of view-specific predictions and adjusts the final predictions according to the degree of trust.

**Trusted Multi-View Classification** has emerged as a crucial area and a pivotal domain within Multi-View Learning. This research area aims to enhance the accuracy and dependability of classification models by integrating data from multiple views, guided by their prediction confidence and epistemic uncertainty. The seminal work, Trusted Multi-View Classification (TMC) [8], introduced the fusion of different views from an opinion perspective using the Dempster-Shafer Combination rule. Building

Table 2: Top-1 accuracy on test split.

Dataset	Handwritten	Caltech101	PIE	Scene15	HMDB	CUB	AVG
F-Mode	99.10±0.20	94.13±0.08	79.41±0.00	62.45±0.11	51.70±0.41	70.25±0.38	76.13
F-Avg	99.25±0.00	<b>95.59±0.06</b>	90.59±0.29	76.21±0.09	71.49±0.35	92.75±0.53	87.65
MGP	99.60±0.10	94.42±0.20	90.13±0.87	74.30±0.41	73.97±0.15	90.79±1.03	87.03
ECML	99.57±0.11	94.25±0.08	91.40±0.47	64.34±0.11	72.90±0.11	92.58±0.25	85.84
TMC	99.63±0.13	94.30±0.13	87.43±0.90	73.99±0.19	73.30±0.18	92.50±0.37	86.60
TF(ours)	99.68±0.11	<u>95.26±0.10</u>	<u>93.31±0.40</u>	<u>77.83±0.32</u>	<u>74.35±0.09</u>	<u>93.33±0.75</u>	<u>88.96</u>
ETMC	<u>99.75±0.00</u>	94.41±0.11	91.69±0.47	<u>78.41±0.20</u>	74.01±0.19	<u>93.67±0.41</u>	88.74
ETF(ours)	<b>99.98±0.07</b>	95.07±0.08	<b>94.63±0.34</b>	<b>82.01±0.17</b>	<b>75.55±0.15</b>	<b>94.08±0.38</b>	<b>90.22</b>

upon TMC, [9] extended the approach by incorporating the pseudo-view, a concatenation of all other views, resulting in improved performance. Subsequent studies by [25] and [36] explored alternative opinion fusion methods. Concurrent research efforts, such as those by [19] and [20], focus on multiview uncertainty estimation, enhancing the model’s reliability.

**Confictive Multi-View Classification** argues that existing work primarily focusing on either learning joint aligned representations or better quantifying uncertainty overlook the problem of potential contradictory in the prediction space. Recognizing this gap, the pioneer work by [36] highlighted this issue and introduced the Degree of Conflict loss. This loss quantifies the disparity between different predictions in the prediction space while accounting for uncertainty, aiming to mitigate conflict-related challenges. However, this approach may inadvertently lead correct predictions to converge towards incorrect ones, potentially jeopardizing model stability. In contrast, our method can generate more accurate predictions with properly estimated uncertainty.

## 4 Experiments

### 4.1 Experimental Setup

**Datasets.** Following [8, 9, 19, 36], we conducted experiments on six benchmark datasets: Handwritten,<sup>5</sup> Caltech101 [4], PIE,<sup>6</sup> Scene15 [3], HMDB [23] and CUB [32] with train-test split of 80% vs. 20%. As we utilized the exact same datasets, we direct readers to [8] for further details regarding these datasets. A summary of these datasets is provided in the Appendix A.7.

**Baseline Methods.** We aim to resolve conflicts among predictions of different views, so we consider the methods that generate view-specific predictions which could have potential conflicts, and thus included following baselines: Fusion by Majority Voting (F-Mode) and Fusion by Probability Averaging (F-Avg), which are two commonly used fusion methods in most MVC methods. We also consider existing trust-worthy baselines, MGP [19] TMC [8], and the conflict resolution pioneering work ECML [36]. Our method can be extended to leverage the pseudo view, as demonstrated by its application to ETMC [9], an extended version of TMC that incorporates pseudo views. All methods were run on a single 24GB RTX3090 card for fair comparison.

### 4.2 Experiment Results and Analysis

We compared our method with baselines with different metrics. For each individual metric, mean and standard deviation from ten runs with different random seeds are reported. In all tables, the best-performing method is highlighted in bold, and the second-best method is underlined.

**Prediction Accuracy.** Similar to [8, 9, 19, 36], we first evaluated the model performance on the test split by Top-1 Classification Accuracy, as shown in Table 2. Building on the strengths of pseudo view, our method (ETF) consistently outperforms all trustworthy-based methods, and gains the best average performance over six datasets compared with all baselines. For example, on the PIE and Scene15 datasets, the use of trust boosts the accuracy of ETMC by 2.94% and 3.60%, respectively. Moreover, ETF surpasses the pioneering conflict resolving method ECML by a substantial margin of 3.23% on PIE, 9.66% on Scene15 and 2.65% on HMDB, highlighting better power of conflicts handling of our method. It is worth noting that Caltech101 inherently has lower level of conflicts, as

<sup>5</sup><https://archive.ics.uci.edu/ml/datasets/Multiple+Features>

<sup>6</sup><http://www.cs.cmu.edu/afs/cs/project/PIE/MultiPie/Multi-Pie/Home.html>

Table 3: Fleiss’ Kappa on test splits.

Dataset	Handwritten	Caltech101	PIE	Scene15	HMDB	CUB	AVG
F-Mode	0.63±0.04	<b>0.97±0.00</b>	0.38±0.00	<u>0.42±0.00</u>	<u>0.56±0.00</u>	<b>0.71±0.01</b>	<u>0.61</u>
F-Avg	0.54±0.03	<b>0.97±0.00</b>	0.37±0.01	<u>0.42±0.00</u>	0.55±0.01	0.58±0.06	0.57
MGP	0.59±0.05	0.94±0.00	0.21±0.01	0.33±0.00	0.51±0.00	0.43±0.07	0.50
ECML	0.42±0.05	<u>0.95±0.00</u>	<u>0.40±0.01</u>	0.26±0.00	0.53±0.01	0.44±0.07	0.50
TMC	0.54±0.07	0.94±0.01	0.23±0.02	0.30±0.01	0.52±0.01	0.37±0.19	0.48
TF(ours)	<u>0.65±0.02</u>	<u>0.95±0.00</u>	0.36±0.01	0.39±0.00	0.54±0.00	0.51±0.10	0.57
ETMC	0.66±0.01	0.84±0.00	0.28±0.04	0.37±0.00	-0.15±0.04	0.45±0.10	0.41
ETF(ours)	<b>0.76±0.02</b>	<u>0.95±0.00</u>	<b>0.48±0.01</b>	<b>0.48±0.01</b>	<b>0.65±0.00</b>	<u>0.64±0.03</u>	<b>0.66</b>

Table 4: MVAGT on test split.

Dataset	Handwritten	Caltech101	PIE	Scene15	HMDB	CUB
F-Mode	88.87±1.73	<u>94.13±0.08</u>	79.41±0.00	62.54±0.11	51.70±0.41	70.25±0.38
F-Avg	18.78±5.89	93.89±0.24	17.06±1.22	27.70±0.36	51.18±0.51	59.50±5.25
MGP	81.37±5.73	91.55±0.29	63.20±2.31	52.10±0.41	50.43±0.42	42.50±9.26
ECML	74.08±0.61	91.05±0.27	78.46±1.19	41.91±0.31	50.95±0.48	48.58±5.36
TMC	81.58±6.57	90.27±0.38	51.54±3.00	51.42±0.46	50.37±0.45	43.25±14.8
TF(ours)	88.97±0.61	<u>92.01±0.22</u>	<u>80.59±0.75</u>	60.41±0.52	<u>52.47±0.35</u>	54.33±7.54
ETMC	<u>98.10±0.17</u>	92.41±0.32	75.15±4.13	<u>73.75±0.45</u>	8.45±1.09	91.08±1.06
ETF(ours)	<b>98.53±0.08</b>	<b>94.47±0.12</b>	<b>90.37±0.40</b>	<b>79.18±0.38</b>	<b>71.43±0.32</b>	<b>91.17±0.67</b>

corroborated by high accuracy and Fleiss’ Kappa scores (Table 3) of all baselines. Nevertheless, ETF maintains the compatible performance with the best one, F-Avg (a minor decrease of 0.52%), and still outperforms other trustworthy methods, e.g., improve the accuracy of ETMC by 0.66%.

When compared to well-established trustworthy methods like TMC, MGP, and ECML without pseudo views, our method TF consistently demonstrates superior performance across all datasets. For example, our proposed trust discounting method enhance TMC’s performance by 3.84% on Scene15 and 5.88% on PIE, while also achieving the highest Top-1 accuracy on other datasets. Notably, our method TF, even without incorporating pseudo views, exhibits comparable performance to ETMC with pseudo views. For instance, TF outperforms ETMC on three datasets (Caltech101, PIE, and HMDB) out of a total of six.

**Reliable Prediction.** To further validate the effectiveness of our proposed method, we evaluate it with two additional metrics, Fleiss’ Kappa [6] and our proposed metric, Multi-View Agreement with Ground Truth (MVAGT). Fleiss’ Kappa is a statistical measure for assessing the reliability of agreement between different raters, with scores closer to 1 indicating higher agreement among the different predictions. As depicted in Table 3, our method (ETF) achieves the highest Fleiss’ Kappa score on four datasets (Handwritten, PIE, Scene15, HMDB and CUB). Even through ETF does not rank first on the remaining two datasets (the third on Caltech101 and the second on CUB), it remains the most generalizable model with the highest average Fleiss’ Kappa (0.66). It’s worth noting that while our method assumes the existence of conflicts, Caltech101 is a dataset with fewer conflicts, which explains the performance discrepancy in Table 2. Nevertheless, ETF still outperforms other trustworthiness-based methods and enhances the robustness of ETMC with an improvement of approximately 13% on Caltech101. Moreover, it’s essential to highlight that ETMC exhibits extremely poor agreement on HMDB with a negative value of -0.15. However, by applying our method, ETF significantly improves performance by an absolute value of 0.8. This underscores the relative robustness of our method across different datasets.

While a multi-view classification (MVC) classifier with both high accuracy and high Fleiss’ Kappa score generally suggests good reliability, high Fleiss’ Kappa scores without reference to the ground truth label might be misleading, particularly in cases where the majority of views agree on the same incorrect class. Therefore, we propose a new evaluation metric (MVAGT), specifically tailored for conflict MVC scenarios. MVAGT assesses correctness on the test split by verifying that more than half of the views make correct decisions. Since majority agreement is often more reasonable for final decisions in real-world scenarios, evaluating methods using MVAGT ensures the reasonableness of the fused decision. Further details about MVAGT are provided in Appendix A.6. As depicted in Table. 4, ETF demonstrates superior performance compared to other methods. Moreover, ETF exhibits



Table 5: AUC-ROC scores for identifying incorrect predictions using uncertainty scores.

Dataset	Handwritten	Caltech101	PIE	Scene15	HMDB	CUB
MGP	99.29±0.30	87.62±0.90	88.43±0.67	63.92±1.96	82.87±0.60	58.20±11.4
ECML	79.05±5.62	86.31±0.50	87.51±0.49	60.50±0.25	81.63±0.15	57.30±8.50
TMC	99.23±0.22	87.33±0.47	90.16±0.99	62.60±0.54	82.63±0.48	64.80±10.5
TF(ours)	99.32±0.35	<b>88.99±0.54</b>	<b>95.90±0.08</b>	64.56±2.02	83.59±0.23	53.52±14.3
ETMC	99.30±0.19	88.35±0.63	93.02±1.40	66.49±0.44	85.42±0.34	<b>72.56±8.11</b>
ETF(ours)	<b>99.90±0.30</b>	88.70±0.54	92.47±1.19	<b>70.44±1.10</b>	<b>86.23±0.49</b>	64.41±3.54

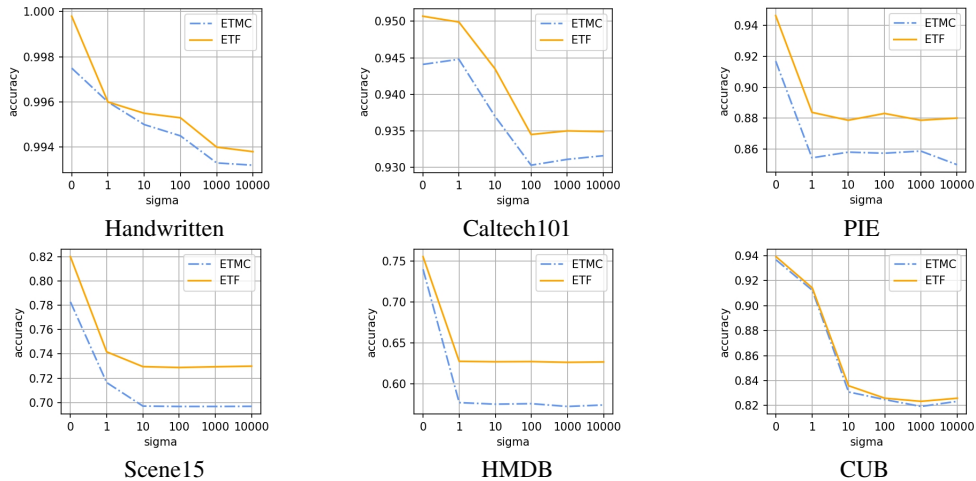


Figure 3: Performance comparison of simulated conflict predictions.

good generalizability across different datasets, where ETMC experiences significant decreases (e.g., HMDB) or other methods alternately occupy the second-best position.

**AUC-ROC for Uncertainty-Aware Prediction.** Following prior work [5], we assess uncertainty by approaching it as the task of determining whether to trust the model’s prediction, evaluating the model’s ability to identify incorrect predictions based on uncertainty scores. Specifically, we employed AUC-ROC to measure the model’s discriminate power in distinguishing incorrect predictions using uncertainty scores. As shown in Table 5, TF and ETF consistently demonstrate the best performance in uncertainty-based classification across five out of the six datasets, showcasing their robust generalizability. Despite a slight performance decrease on the CUB dataset, our method (ETF) still maintains the second-best result, outperforming other approaches, whether incorporating pseudo views or not. One possible reason for the decrease is that our method may increase the belief mass of ground truth label for some incorrectly predicted instances, thus correcting the incorrect predictions. However, the decrease in uncertainty is relatively small (e.g., 0.5 for incorrect changes to 0.4 for correct). An example is shown in the Appendix B.2.

**Simulating Conflicting Predictions with Noisy Instances.** Following a similar approach as [8, 19, 36], we introduce varying levels of Gaussian noise (e.g., with standard deviations of 10 and 100) to randomly selected half of the views for each instance in the dataset, creating noisy views. The original views are then replaced by these noisy views, and the model is trained using the updated dataset. Consequently, the model’s predictions based on the noisy views may conflict with the predictions from the views without explicitly introducing noise. As illustrated in Figure 3 and Appendix B.3, our methods (ETF and TF) consistently outperform others with or without pseudo views, demonstrating the effectiveness of TD and our training algorithm’s ability to handle conflicting views.

## 5 Conclusion

In this paper, we introduced a theoretically-funded approach for resolving conflicts in Multi-View Classification. This approach is built on top of the principle of trust discounting in Subjective Logic, where the computational trust, aka referral trust, is represented as a Binomial opinion with a Beta

probability density function. The functional trust is then discounted by the amount computed as a function of the degree of trust. We demonstrated through extensive experiments that the proposed trust discounting method not only benefits classification accuracy but also increases consistency among different views, providing a new reliable approach to handling conflicts in MVC. A possible limitation of our work is that the warm-up loss is not optimal solution. We leave it for future work.

## References

- [1] Pradeep K Atrey, M Anwar Hossain, Abdulmotaleb El Saddik, and Mohan S Kankanhalli. Multimodal fusion for multimedia analysis: a survey. *Multimedia systems*, 16:345–379, 2010.
- [2] Marco Federici, Anjan Dutta, Patrick Forré, Nate Kushman, and Zeynep Akata. Learning robust representations via multi-view information bottleneck. In *International Conference on Learning Representations*, 2020.
- [3] Li Fei-Fei and Pietro Perona. A bayesian hierarchical model for learning natural scene categories. In *Computer Society Conference on Computer Vision and Pattern Recognition*, volume 2, pages 524–531, 2005.
- [4] Li Fei-Fei, Rob Fergus, and Pietro Perona. Learning generative visual models from few training examples: An incremental bayesian approach tested on 101 object categories. In *Conference on Computer Vision and Pattern Recognition workshop*, pages 178–178, 2004.
- [5] Angelos Filos, Sebastian Farquhar, Aidan N Gomez, Tim GJ Rudner, Zachary Kenton, Lewis Smith, Milad Alizadeh, Arnoud de Kroon, and Yarin Gal. A systematic comparison of bayesian deep learning robustness in diabetic retinopathy tasks. *arXiv preprint arXiv:1912.10481*, 2019.
- [6] Joseph L Fleiss. Measuring nominal scale agreement among many raters. *Psychological bulletin*, 76(5):378, 1971.
- [7] Ian Goodfellow, Jean Pouget-Abadie, Mehdi Mirza, Bing Xu, David Warde-Farley, Sherjil Ozair, Aaron Courville, and Yoshua Bengio. Generative adversarial networks. *Communications of the ACM*, 63(11):139–144, 2020.
- [8] Zongbo Han, Changqing Zhang, Huazhu Fu, and Joey Tianyi Zhou. Trusted multi-view classification. In *International Conference on Learning Representations*, 2021.
- [9] Zongbo Han, Changqing Zhang, Huazhu Fu, and Joey Tianyi Zhou. Trusted multi-view classification with dynamic evidential fusion. *IEEE transactions on pattern analysis and machine intelligence*, 45(2):2551–2566, 2022.
- [10] David R Hardoon, Sandor Szedmak, and John Shawe-Taylor. Canonical correlation analysis: An overview with application to learning methods. *Neural computation*, 16(12):2639–2664, 2004.
- [11] R Devon Hjelm, Alex Fedorov, Samuel Lavoie-Marchildon, Karan Grewal, Phil Bachman, Adam Trischler, and Yoshua Bengio. Learning deep representations by mutual information estimation and maximization. In *International Conference on Learning Representations*, 2019.
- [12] Dongdong Hou, Yang Cong, Gan Sun, Jiahua Dong, Jun Li, and Kai Li. Fast multi-view outlier detection via deep encoder. *IEEE Transactions on Big Data*, 8(4):1047–1058, 2020.
- [13] Zhenyu Huang, Peng Hu, Joey Tianyi Zhou, Jiancheng Lv, and Xi Peng. Partially view-aligned clustering. *Advances in Neural Information Processing Systems*, 33:2892–2902, 2020.
- [14] Zongmo Huang, Yazhou Ren, Xiaorong Pu, Shudong Huang, Zenglin Xu, and Lifang He. Self-supervised graph attention networks for deep weighted multi-view clustering. In *Proceedings of the AAAI Conference on Artificial Intelligence*, volume 37, pages 7936–7943, 2023.
- [15] Audun Jøsang. *Subjective Logic: A formalism for reasoning under uncertainty*. Springer Publishing Company, Incorporated, 2018.
- [16] Audun Jøsang, Tanja Ažderska, and Stephen Marsh. Trust transitivity and conditional belief reasoning. In *Trust Management VI: 6th IFIP WG 11.11 International Conference, IFIPTM 2012, Surat, India, May 21-25, 2012. Proceedings 6*, pages 68–83, 2012.
- [17] Audun Jøsang, Paulo CG Costa, and Erik Blasch. Determining model correctness for situations of belief fusion. In *Proceedings of the 16th International Conference on Information Fusion*, pages 1886–1893, 2013.

- [18] Audun Jøsang, Magdalena Ivanovska, and Tim Muller. Trust revision for conflicting sources. In *2015 18th International Conference on Information Fusion (Fusion)*, pages 550–557, 2015.
- [19] Myong Chol Jung, He Zhao, Joanna Dipnall, Belinda Gabbe, and Lan Du. Uncertainty estimation for multi-view data: the power of seeing the whole picture. *Advances in Neural Information Processing Systems*, 35:6517–6530, 2022.
- [20] Myong Chol Jung, He Zhao, Joanna Dipnall, and Lan Du. Beyond unimodal: Generalising neural processes for multimodal uncertainty estimation. *Advances in Neural Information Processing Systems*, 36, 2023.
- [21] Hengyuan Kang, Liming Xia, Fuhua Yan, Zhibin Wan, Feng Shi, Huan Yuan, Huiting Jiang, Dijia Wu, He Sui, Changqing Zhang, et al. Diagnosis of coronavirus disease 2019 (covid-19) with structured latent multi-view representation learning. *IEEE transactions on medical imaging*, 39(8):2606–2614, 2020.
- [22] Diederik Kingma and Jimmy Ba. Adam: A method for stochastic optimization. In *International Conference on Learning Representations (ICLR)*, 2015.
- [23] Hildegard Kuehne, Hueihan Jhuang, Estíbaliz Garrote, Tomaso Poggio, and Thomas Serre. Hmdb: a large video database for human motion recognition. In *2011 International Conference on Computer Vision*, pages 2556–2563, 2011.
- [24] Paul Pu Liang, Amir Zadeh, and Louis-Philippe Morency. Foundations and trends in multimodal machine learning: Principles, challenges, and open questions. *ACM Comput. Surv.*, 2024.
- [25] Wei Liu, Xiaodong Yue, Yufei Chen, and Thierry Denoëux. Trusted multi-view deep learning with opinion aggregation. In *Proceedings of the AAAI Conference on Artificial Intelligence*, volume 36, pages 7585–7593, 2022.
- [26] Rafael Müller, Simon Kornblith, and Geoffrey E Hinton. When does label smoothing help? *Advances in neural information processing systems*, 32, 2019.
- [27] Mohammad Taghi Niknejad. Scaphoid fracture - Case Study. <https://radiopaedia.org/cases/99029>, 2022.
- [28] Adam Paszke, Sam Gross, Francisco Massa, Adam Lerer, James Bradbury, Gregory Chanan, Trevor Killeen, Zeming Lin, Natalia Gimelshein, Luca Antiga, Alban Desmaison, Andreas Kopf, Edward Yang, Zachary DeVito, Martin Raison, Alykhan Tejani, Sasank Chilamkurthy, Benoit Steiner, Lu Fang, Junjie Bai, and Soumith Chintala. Pytorch: An imperative style, high-performance deep learning library. *Advances in Neural Information Processing Systems*, 32, 2019.
- [29] Murat Sensoy, Lance Kaplan, and Melih Kandemir. Evidential deep learning to quantify classification uncertainty. *Advances in neural information processing systems*, 31, 2018.
- [30] Glenn Shafer. *A mathematical theory of evidence*, volume 42. Princeton university press, 1976.
- [31] Amin Tafti and Doug W Byerly. X-ray radiographic patient positioning. *StatPearls*, 2020.
- [32] C Wah, S Branson, P Welinder, P Perona, and S Belongie. The Caltech-UCSD Birds-200-2011 dataset. Technical report, California Institute of Technology, 2011.
- [33] Weiran Wang, Raman Arora, Karen Livescu, and Jeff Bilmes. On deep multi-view representation learning. In *International conference on machine learning*, pages 1083–1092. PMLR, 2015.
- [34] Jie Wen, Chengliang Liu, Gehui Xu, Zhihao Wu, Chao Huang, Lunke Fei, and Yong Xu. Highly confident local structure based consensus graph learning for incomplete multi-view clustering. In *Proceedings of the IEEE/CVF Conference on Computer Vision and Pattern Recognition*, pages 15712–15721, 2023.
- [35] Yi Wen, Siwei Wang, Qing Liao, Weixuan Liang, Ke Liang, Xinhang Wan, and Xinwang Liu. Unpaired multi-view graph clustering with cross-view structure matching. *IEEE Transactions on Neural Networks and Learning Systems*, 2023.

- [36] Cai Xu, Jiajun Si, Ziyu Guan, Wei Zhao, Yue Wu, and Xiyue Gao. Reliable conflictive multi-view learning. *Proceedings of the AAAI Conference on Artificial Intelligence*, 38:16129–16137, 2024.
- [37] Ekim Yurtsever, Jacob Lambert, Alexander Carballo, and Kazuya Takeda. A survey of autonomous driving: Common practices and emerging technologies. *IEEE access*, 8:58443–58469, 2020.
- [38] Changqing Zhang, Yeqing Liu, and Huazhu Fu. Ae2-nets: Autoencoder in autoencoder networks. In *Proceedings of the IEEE/CVF conference on computer vision and pattern recognition*, pages 2577–2585, 2019.
- [39] Chaoyang Zhang, Zhengzheng Lou, Qinglei Zhou, and Shizhe Hu. Multi-view clustering via triplex information maximization. *IEEE Transactions on Image Processing*, 2023.
- [40] Pei Zhang, Siwei Wang, Liang Li, Changwang Zhang, Xinwang Liu, En Zhu, Zhe Liu, Lu Zhou, and Lei Luo. Let the data choose: Flexible and diverse anchor graph fusion for scalable multi-view clustering. In *Proceedings of the AAAI Conference on Artificial Intelligence*, volume 37, pages 11262–11269, 2023.
- [41] Lecheng Zheng, Yu Cheng, Hongxia Yang, Nan Cao, and Jingrui He. Deep co-attention network for multi-view subspace learning. In *Proceedings of the Web Conference 2021*, pages 1528–1539, 2021.

## A Proofs and Derivations

### A.1 Calculation of Predictive Probability

According to Subjective Logic (SL) [15], the predictive probability  $p_k$  for class  $k$ , can be calculated by

$$p_k = b_k + a_k * u \quad (9)$$

where  $b_k$  is the belief mass for  $k$ -th label,  $u$  is the predictive uncertainty or epistemic uncertainty [29]. We usually assume the prior  $a_k$  conforms to a uniform discrete distribution, i.e.,  $a_k = 1/K$ .

Above equation is identical to

$$p_k = \frac{\alpha_k}{S} \quad (10)$$

where  $\alpha_k$  is the Dirichlet concentration parameter for  $k$ -th label, and  $S$  is the Dirichlet strength, i.e.,  $S = \sum_k \alpha_k$ .

*Proof.*

$$\begin{aligned} p_k &= b_k + a_k * u \\ &= b_k + \frac{1}{K} * \frac{K}{S} \\ &= \frac{e_k}{S} + \frac{1}{S} \\ &= \frac{\alpha_k}{S} \end{aligned}$$

□

Since Beta Distribution is 2-dimensional Dirichlet Distribution, above equations for calculating probabilities of multinomial opinions could also be applied to binomial opinions.

### A.2 Alternative Representation of Belief Constraint Fusion(BCF)

*Proof.* We the proof for Eq. (3) as follows,

$$\begin{aligned} e_k &= S * b_k \\ &= S \frac{1}{1-C} (b_k^1 b_k^2 + b_k^1 u^2 + b_k^2 u^1) \\ &= S \frac{1 - \sum_k b_k}{u^1 u^2} (b_k^1 b_k^2 + b_k^1 u^2 + b_k^2 u^1) \\ &= (S - S * \sum_k b_k) \frac{1}{u^1 u^2} (b_k^1 b_k^2 + b_k^1 u^2 + b_k^2 u^1) \\ &= (S - \sum_k e_k) \frac{1}{u^1 u^2} (b_k^1 b_k^2 + b_k^1 u^2 + b_k^2 u^1) \\ &= K \frac{1}{u^1 u^2} (b_k^1 b_k^2 + b_k^1 u^2 + b_k^2 u^1) \\ &= K \frac{1}{u^1 u^2} \left( \frac{e_k^1 e_k^2}{S^1 S^2} + \frac{e_k^1 u^2}{S^1} + \frac{e_k^2 u^1}{S^2} \right) \\ &= K \left( \frac{e_k^1 e_k^2}{K * K} + \frac{e_k^1 u^2}{K u^2} + \frac{e_k^2 u^1}{K u^1} \right) \\ &= \frac{e_k^1 e_k^2}{K} + e_k^1 + e_k^2 \end{aligned}$$

□

### A.3 Dirichlet Evidence Updating by Trust Discounting (TD)

As mentioned earlier, the TD in Definition 2 is corresponds to update Dirichlet evidence using following equation,

$$\check{e}_k = \frac{\check{p}_t \check{u}}{1 - \check{p}_t + \check{p}_t \check{u}} \acute{e}_k \quad (11)$$

where  $\check{p}_t$  is the probability representing trust degree and  $\check{u}$  is the uncertainty for functional opinion.  $\acute{e}_k$  is Dirichlet evidence of functional opinion, and  $\check{e}_k$  is Dirichlet evidence after discounting.

*Proof.*

$$\begin{aligned} \check{e}_k &= \check{\mathbf{b}}_k * \check{S} \\ &= \frac{\check{p}_t \acute{b}_k K}{\check{u}} \\ &= \frac{\check{p}_t \acute{b}_k K}{1 - \check{p}_t + \check{p}_t \check{u}} \\ &= \frac{\check{p}_t}{1 - \check{p}_t + \check{p}_t \check{u}} \frac{\acute{e}_k}{\check{S}} K \\ &= \frac{\check{p}_t}{1 - \check{p}_t + \check{p}_t \check{u}} \frac{K}{\check{S}} \acute{e}_k \\ &= \frac{\check{p}_t \check{u}}{1 - \check{p}_t + \check{p}_t \check{u}} \acute{e}_k \end{aligned}$$

□

### A.4 Detailed Proof of Propositions

*Proof.* Proof details of Proposition 1. We use  $g$  to denote the index of ground-truth label. Recall that scalar probability  $\check{p}_t$  represents the degree of trust as mentioned before. With at least one view's prediction is correct, the belief mass of ground truth label of BCF combined opinion, which integrates through trust-discounted opinions, is as follows,

$$\begin{aligned} \bar{b}_g &= \frac{1}{1 - \check{C}} (\check{b}_g^1 \check{b}_g^2 + \check{b}_g^1 \check{u}^2 + \check{b}_g^2 \check{u}^1) \\ &= \frac{1}{1 - \check{C}} ((\check{b}_g^1 \check{p}_t^1)(\check{b}_g^2 \check{p}_t^2) + \check{b}_g^1 \check{p}_t^1 \check{u}^2 + \check{b}_g^2 \check{p}_t^2 \check{u}^1) \end{aligned}$$

And we have the discounted uncertainty

$$\begin{aligned} \check{u} &= 1 - \check{p}_t \left( \sum_k \acute{b}_k \right) \\ &= 1 - \check{p}_t (1 - \acute{u}) \\ &= 1 - \check{p}_t + \check{p}_t * \acute{u} \end{aligned}$$

In cases where the belief mass of the ground truth label is maximal (i.e., predicted label is the ground truth label), our referral network should generate a high trust value, that is  $\check{p}_t \rightarrow 1$  when  $\acute{b}_g = \max(\acute{\mathbf{b}})$ , and otherwise  $\check{p}_t \rightarrow 0$ . Therefore,  $\check{u} \rightarrow \acute{u}$  when  $\acute{b}_g = \max(\acute{\mathbf{b}})$ , and  $\check{u} \rightarrow 1$  as well. Therefore, the fused term will be dominant by correctly predicted views as  $\check{p}_t \rightarrow 1$  as well as  $\check{u} \rightarrow 1$  which contributes in cross multiplication. Subsequently,

$$\begin{aligned} \bar{b}_g &= \frac{1}{1 - \check{C}} ((\check{b}_g^1 \check{p}_t^1)(\check{b}_g^2 \check{p}_t^2) + \check{b}_g^1 \check{p}_t^1 \check{u}^2 + \check{b}_g^2 \check{p}_t^2 \check{u}^1) \\ &\geq \frac{1}{1 - \check{C}} ((\check{b}_k^1 \check{p}_t^1)(\check{b}_k^2 \check{p}_t^2) + \check{b}_k^1 \check{p}_t^1 \check{u}^2 + \check{b}_k^2 \check{p}_t^2 \check{u}^1) \text{ (equality holds iif. } k = z) \\ &= \frac{1}{1 - \check{C}} (\check{b}_k^1 \check{b}_k^2 + \check{b}_k^1 \check{u}^2 + \check{b}_k^2 \check{u}^1) = \bar{b}_k \end{aligned}$$

□

*Proof.* Proof details of Proposition 2. Let  $\bar{u}$  and  $\bar{u}'$  denote the uncertainty of BCF combined opinion with or without Trust Discounting, respectively.

$$\begin{aligned}
\bar{u} &= \frac{1}{\sum_{k=1}^K \left( \frac{\hat{b}_k^1 \hat{b}_k^2}{\hat{u}^1 \hat{u}^2} + \frac{\hat{b}_k^1}{\hat{u}^1} + \frac{\hat{b}_k^2}{\hat{u}^2} \right) + 1} \\
&= \frac{1}{\sum_{k=1}^K \left( \frac{\hat{b}_k^1 \hat{p}_t^1 \hat{b}_k^2 \hat{p}_t^2}{(\hat{u}^1 \hat{p}_t^1 + 1 - \hat{p}_t^1)(\hat{u}^2 \hat{p}_t^2 + 1 - \hat{p}_t^2)} + \frac{\hat{b}_k^1 \hat{p}_t^1}{\hat{u}^1 \hat{p}_t^1 + 1 - \hat{p}_t^1} + \frac{\hat{b}_k^2 \hat{p}_t^2}{\hat{u}^2 \hat{p}_t^2 + 1 - \hat{p}_t^2} \right) + 1} \\
&= \frac{1}{\sum_{k=1}^K \left( \frac{\hat{b}_k^1 \hat{b}_k^2}{\left( \frac{\hat{u}^1}{\hat{p}_t^1} + \frac{1}{\hat{p}_t^1 \hat{p}_t^2} - \frac{1}{\hat{p}_t^2} \right) \left( \frac{\hat{u}^2}{\hat{p}_t^2} + \frac{1}{\hat{p}_t^1 \hat{p}_t^2} - \frac{1}{\hat{p}_t^1} \right)} + \frac{\hat{b}_k^1}{\hat{u}^1 + \frac{1}{\hat{p}_t^1} - 1} + \frac{\hat{b}_k^2}{\hat{u}^2 + \frac{1}{\hat{p}_t^2} - 1} \right) + 1} \\
&= \frac{1}{\sum_{k=1}^K \left( \frac{\hat{b}_k^1 \hat{b}_k^2}{\left( \frac{\hat{u}^1}{\hat{p}_t^2} + \frac{1 - \hat{p}_t^1}{\hat{p}_t^1 \hat{p}_t^2} \right) \left( \frac{\hat{u}^2}{\hat{p}_t^1} + \frac{1 - \hat{p}_t^2}{\hat{p}_t^1 \hat{p}_t^2} \right)} + \frac{\hat{b}_k^1}{\hat{u}^1 + \frac{1}{\hat{p}_t^1} - 1} + \frac{\hat{b}_k^2}{\hat{u}^2 + \frac{1}{\hat{p}_t^2} - 1} \right) + 1} \\
&\geq \frac{1}{\sum_{k=1}^K \left( \frac{\hat{b}_k^1 \hat{b}_k^2}{\hat{u}^1 \hat{u}^2} + \frac{\hat{b}_k^1}{\hat{u}^1} + \frac{\hat{b}_k^2}{\hat{u}^2} \right) + 1} = \bar{u}'
\end{aligned}$$

□

## A.5 Loss Functions and Hyperparameters for Optimization

Recall that the probability density function (pdf) of the Dirichlet distribution,  $\text{Dir}(\mathbf{p} \mid \boldsymbol{\alpha})$ , is given by:

$$\text{Dir}(\mathbf{p} \mid \boldsymbol{\alpha}) = \frac{1}{B(\boldsymbol{\alpha})} \prod_{i=1}^K p_i^{\alpha_i - 1}$$

where:

- $\mathbf{p} = (p_1, p_2, \dots, p_K)$  is a probability vector, such that  $\sum_{k=1}^K p_k = 1$  and  $p_k \geq 0$  for all  $k$ .
- $\boldsymbol{\alpha} = (\alpha_1, \alpha_2, \dots, \alpha_K)$  is a vector of concentration parameters, with  $\alpha_k > 0$ .
- $B(\boldsymbol{\alpha})$  is the multivariate Beta function, defined as  $B(\boldsymbol{\alpha}) = \frac{\prod_{k=1}^K \Gamma(\alpha_k)}{\Gamma(\sum_{k=1}^K \alpha_k)}$ .
- $\Gamma(\cdot)$  is the Gamma function.

Our loss function for Dirichlet Parameters  $\boldsymbol{\alpha}$  is

$$L(\boldsymbol{\alpha}) = L_{ace}(\boldsymbol{\alpha}) + \lambda D_{KL}[\text{Dir}(\mathbf{p} \mid \tilde{\boldsymbol{\alpha}}) \parallel \text{Dir}(\mathbf{p} \mid \mathbf{1})] \quad (12)$$

Recall that  $\tilde{\boldsymbol{\alpha}} = \mathbf{y} + (1 - \mathbf{y}) \odot \boldsymbol{\alpha}$  is the Dirichlet parameters after removing non-misleading evidence from predicted parameters  $\boldsymbol{\alpha}$  and  $\mathbf{p}$  is the projected probability, i.e.,  $\mathbf{p} = \frac{\boldsymbol{\alpha}}{S}$ .  $\odot$  is the element-wise product and  $\lambda_o$  is the annealing factor. We follow [29], and use  $\lambda_o = \min(1.0, o/10)$ , where  $o$  is the index of the current epoch.

Specifically, the *ace* loss represents the Bayes risk for Cross-Entropy loss when using a Dirichlet distribution.

$$\begin{aligned}
L_{ace}(\boldsymbol{\alpha}) &= \int \left[ \sum_{k=1}^K -y_k \log(p_k) \right] \frac{1}{B(\boldsymbol{\alpha})} \prod_{k=1}^K (p_k)^{\alpha_k - 1} d\mathbf{p} \\
&= \sum_{k=1}^K y_k (\psi(S) - \psi(\alpha_k))
\end{aligned} \quad (13)$$

Where  $\psi$  is the digamma function.

Recall that our referral network will generate the evidence for binomial opinion, and the evidence will be converted into parameters of Beta Distribution, i.e.,  $Beta(\alpha_0, \alpha_1)$ . Subsequently, by replacing the Dirichlet Distribution with Beta Distribution, and the label  $y_k$  in above equation with another label, we can have the *ace* loss for Beta Distribution, as Eq. (8).



Table 6: TF and ETF hyper-parameters

Hyper-parameter	Handwritten	Caltech101	PIE	Scene15	HMDB	CUB
lr	3e-3	1e-4	3e-3	1e-2	3e-4	1e-3
rlr	3e-4	3e-5	1e-3	3e-3	1e-4	3e-4
weight-decay	1e-4	1e-4	1e-4	1e-4	1e-4	1e-4
warm-up epochs	1	1	1	1	1	1

The KL divergence loss is

$$\begin{aligned}
& D_{KL} [\text{Dir}(\mathbf{p} \mid \boldsymbol{\alpha}) \parallel \text{Dir}(\mathbf{p} \mid \mathbf{1})] \\
&= \log \left( \frac{\Gamma \left( \sum_{k=1}^K \alpha_k \right)}{\Gamma(K) \prod_{k=1}^K \Gamma(\alpha_k)} \right) + \sum_{k=1}^K (\alpha_k - 1) \left[ \psi(\alpha_k) - \psi \left( \sum_{j=1}^K \alpha_j \right) \right] \quad (14)
\end{aligned}$$

The hyper-parameters for training TF and ETF has been shown in in Table 6. Concretely, "lr" is the learning rate for functional networks, "rlr" indicates the learning rate for referral networks. For the "lr", we follow ETMC [9], and used same strategy to select learning rate for the functional nets. When tuning the learning rate for referral networks, we follow a basic principle of starting with a value less than or equal to the base learning rate, and then gradually decreasing the learning rate of referral network by a factor of 3. For fair comparison, we used same learning rate for functional networks for evidence-based methods, except MGP [19], where we followed their paper.

We implement our proposed methods (TF and ETF) using Pytorch (version 1.13) [28] and used Adam optimizer [22] to update network parameters during training on all datasets, with weight decay 1e-4 following [9].

## A.6 Multi-View Agreement with Ground Truth (MVAGT)

The MVAGT (Multi-View Agreement with Ground Truth) is a novel evaluation metric designed specifically for multi-view classification problems with conflicting views. It assesses the model’s performance on the test set by considering the ground truth labels, thus providing a more reliable and realistic measure of the model’s ability to handle view disagreements. The rationality behind MVAGT lies in its alignment with real-world scenarios, where the majority agreement among multiple views is often considered more reasonable for the final decision. In the presence of view conflicts, a model that can make predictions consistent with the majority of views is deemed more trustworthy and reliable. By evaluating models using MVAGT, we can examine the reasonableness of the fused decision and assess the model’s capability to handle view conflicts effectively. Mathematically, MVAGT calculates the accuracy of the model on the test set as follows:

$$\text{MVAGT} = \frac{1}{M} \sum_{i=1}^M \mathbb{1} \left( \sum_{v=1}^V \mathbb{1}((\hat{y}_i^v = y_i) > \frac{V}{2}) \right) \quad (15)$$

where  $M$  is the total number of test samples,  $V$  is the number of views,  $\hat{y}_i^v$  is the predicted label of the  $i$ -th sample from the  $v$ -th view,  $y^i$  is the ground truth label of the  $i$ -th sample, and  $\mathbb{1}(\cdot)$  is the indicator function that returns 1 if the condition is satisfied and 0 otherwise.

Table 7: Summary of Datasets

Dataset	Size	K	Dimensions
HandWritten	2000	10	240/76/216/47/64/6
Caltech101	8677	101	4096/4096
PIE	680	68	484/256/279
Scene15	4485	15	20/59/40
HMDB	6718	51	1000/1000
CUB	600	10	1024/300

## A.7 Summary of Dataset

We provide the summary of the dataset in Table 7, we direct readers to [8] for further details regarding these datasets.

## B Supplementary Insights and Additional Analysis

### B.1 Reduce Conflicts by Trust Fusion

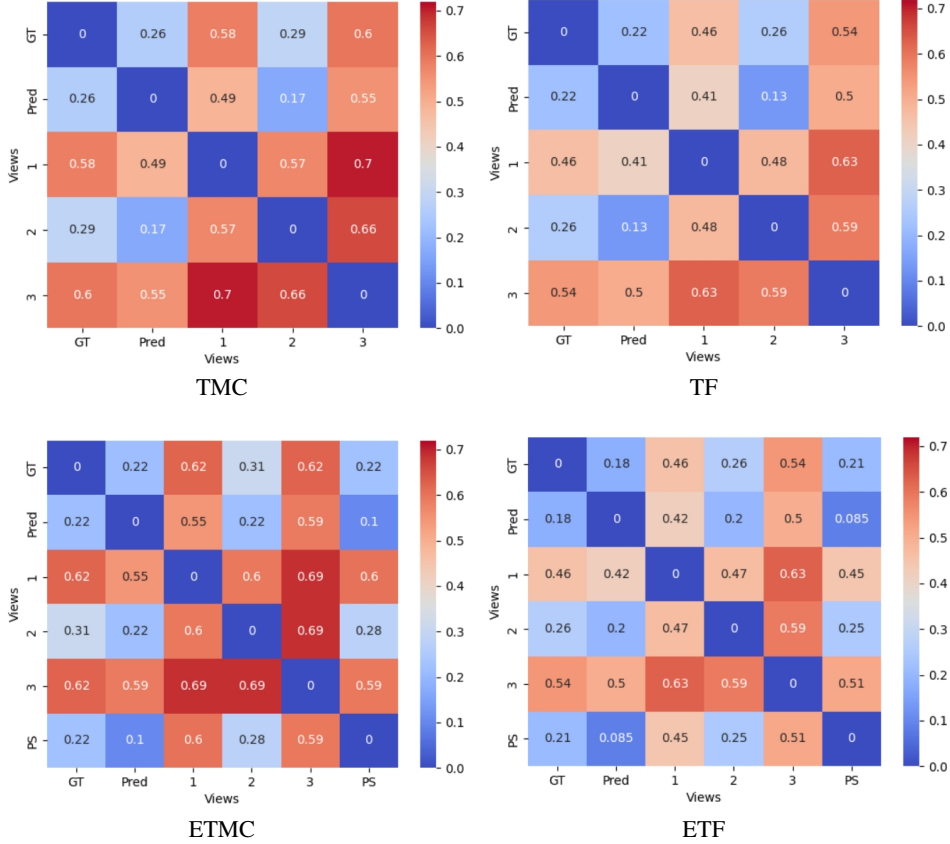


Figure 4: Conflict Ratio on Scene15, Four Methods TMC, TF, ETMC, ETF are compared. GT, Pred, PS are ground-truth view, prediction view, pseudo-view respectively, View 1, 2 and 3 are corresponding to feature view 1, 2 and 3.

We calculate the Conflict Ratio (CR) by normalizing the number of times that the  $v$ -th view prediction is different from  $w$ -th view, i.e.,  $CR(\hat{\mathbf{y}}^v, \hat{\mathbf{y}}^w) = \frac{1}{M} \sum_{i=1}^M \mathbb{1}(\hat{y}_i^v \neq \hat{y}_i^w)$ , where  $M$  is total number of test instances,  $\hat{y}_i^v$  is the predicted label of  $i$ -th instance on  $v$ -th view, and  $\mathbb{1}$  is the indicator function that returns 1 if the condition is satisfied and 0 otherwise. By applying Trust Discounting, both TMC's and ETMC's conflicts between different views are significant reduced. As an example, the CR on Scene15 is visualized by heatmap, shown in Figure 4. The colors in the heatmap generated by our method are noticeably more blue (or less red) than those of the baselines, indicating that the conflict ratio has been reduced by our method.

### B.2 Explanation for the decrease of AUC-ROC for Uncertainty-Aware Prediction on CUB dataset

As the error case displayed in Figure 5, ETF corrects the error prediction made by ETMC. However, even though the combined prediction is correct after applying trust discounting, the predictive uncertainty is still relatively high. If ETF corrects previously incorrect predictions but assigns them

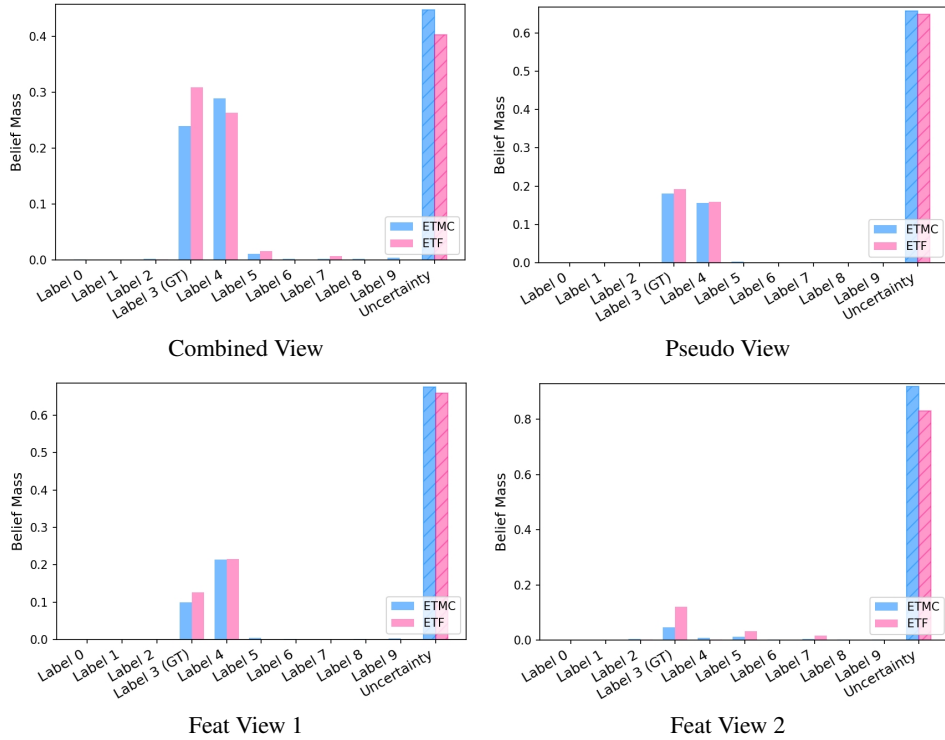


Figure 5: Bar chart for belief mass on each label and predictive uncertainty on one instance of CUB. GT indicates the ground truth label of the selected instance.

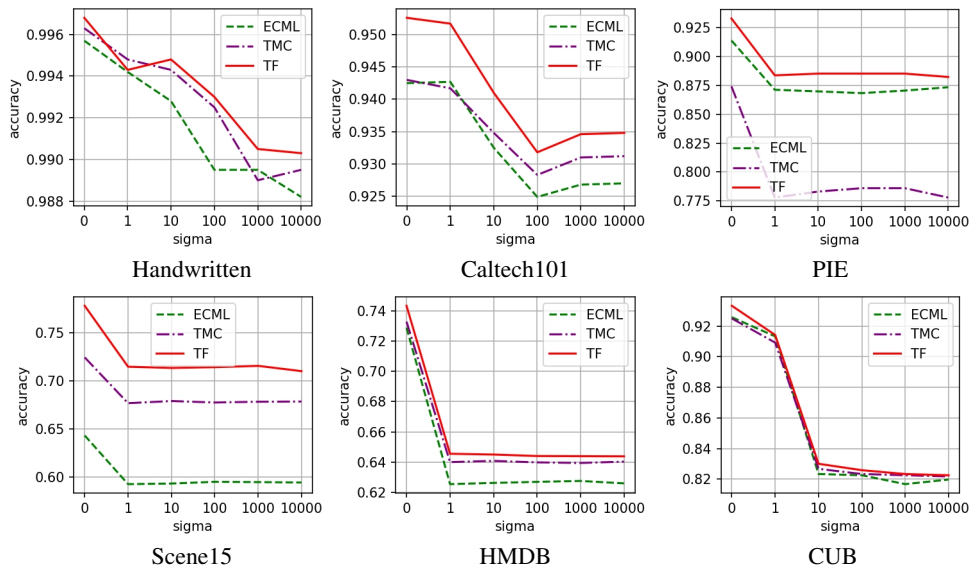


Figure 6: Performance comparison of simulated conflict predictions.

relatively high uncertainty scores (e.g., 0.4), it may lead to a decrease in the AUC-ROC for predictive uncertainty. This is because AUC-ROC evaluates the model's ability to discriminate between correct and incorrect predictions based on uncertainty scores. Correcting predictions while maintaining high uncertainty scores can make it more challenging for the model to distinguish between correct and incorrect predictions, resulting in a lower AUC-ROC score, even though the accuracy improves.

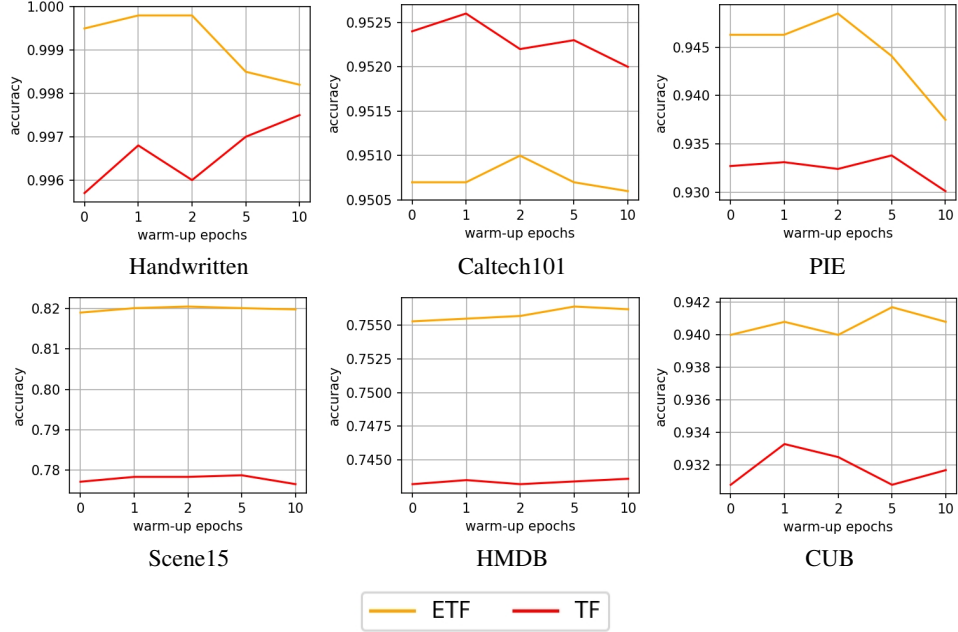


Figure 7: Performance comparison of simulated conflict predictions.

### B.3 Simulating Conflicting Predictions with Noisy Instances

Besides the one we show in Figure 3, we also plot the model performance for evidence-based methods that do not incorporate pseudo views, as shown in Figure 6. Our method TF consistently outperforms other methods like TMC and ECML.

### B.4 Ablation Study of Hyper-parameters

We presented results using a non-over-tuned empirical value of 1 for the hyperparameter ‘warm-up epochs’ in all previous experiments. These results indicated our model’s robust performance, as it consistently outperformed baseline models. Here we demonstrate the effect of this hyperparameter using more finely graded values, starting from 0 (which indicates no warm-up stage) and increasing steadily, for example, to 2, 5, and 10.

From Figure 7, we can find that incorporating warm-up stage (warm-up epochs > 0) can generally results in better model performance. For some datasets (e.g. HMDB), increasing the number of warm-up epochs further improves performance compared to the results previously reported. This observation suggests that adjusting this value based on the specific dataset can lead to enhanced performance.

## C Technical Requirements and Execution

Table 8: Execution Time for ETF and TF on 24GB RTX3090 (Single run)

Method	Handwritten	Caltech101	PIE	Scene15	HMDB	CUB
TF	4min30s	8min40sec	55s	4min50sec	5min30s	40sec
ETF	5min	11min	1min20sec	7min30sec	8min	50sec

### C.1 Execution Time

We report the execution time of single run of the training process, which is shown in Table 8. For example, 1min20sec in the table for ETF on PIE means training ETC on PIE dataset using one 24GB

RTX3090 GPU card will cost about 1 minute and 20 seconds. In our experiment, we will repeat this step 10 time for calculating the mean and standard error.